Discovery of 3,3′-diindolylmethanes as potent antileishmanial agents

ARTICLE *in* EUROPEAN JOURNAL OF MEDICINAL CHEMISTRY · MARCH 2013

Impact Factor: 3.45 · DOI: 10.1016/j.ejmech.2013.02.024

European Journal of Medicinal Chemistry 63 (2013) 435–443

Contents lists available at SciVerse ScienceDirect

European Journal of Medicinal Chemistry

journal homepage: http://www.elsevier.com/locate/ejmech

Original article

Discovery of 3,3′-diindolylmethanes as potent antileishmanial agents☆

Sandip B. Bharate [a,*], Jaideep B. Bharate [a], Shabana I. Khan [b], Babu L. Tekwani [b], Melissa R. Jacob [b], Ramesh Mudududdla [a], Rammohan R. Yadav [a], Baljinder Singh [c], P.R. Sharma [d], Sudip Maity [e], Baldev Singh [c,*], Ikhlas A. Khan [b], Ram A. Vishwakarma [a,c,**]

[a] Medicinal Chemistry Division, Indian Institute of Integrative Medicine (CSIR), Canal Road, Jammu 180001, India
[b] National Centre for Natural Products Research (NCNPR), School of Pharmacy, University of Mississippi, MS 38677, USA
[c] Natural Products Chemistry Division, Indian Institute of Integrative Medicine (CSIR), Canal Road, Jammu 180001, India
[d] Pharmacology Division, Indian Institute of Integrative Medicine (CSIR), Canal Road, Jammu 180001, India
[e] Central Institute of Mining and Fuel Research (CIMFR), Dhanbad, Jharkhand 826001, India

ARTICLE INFO

Article history:
Received 26 December 2012
Received in revised form
20 February 2013
Accepted 22 February 2013
Available online 28 February 2013

Keywords:
3,3′-Diindolylmethanes
Antileishmanial
Antimalarial
Leishmania donovani
Antifungal
Fe-pillared interlayered clay

ABSTRACT

An efficient protocol for synthesis of 3,3′-diindolylmethanes using recyclable Fe-pillared interlayered clay (Fe-PILC) catalyst under aqueous medium has been developed. All synthesized 3,3′-diindolylmethanes showed promising antileishmanial activity against *Leishmania donovani* promastigotes as well as axenic amastigotes. Structure–activity relationship analysis revealed that nitroaryl substituted diindolylmethanes showed potent antileishmanial activity. The 4-nitrophenyl linked 3,3′-diindolylmethane **8g** was found to be the most potent antileishmanial analog showing IC_{50} values of 7.88 and 8.37 μM against both *L. donovani* promastigotes and amastigotes, respectively. Further, a pharmacophore based QSAR model was established to understand the crucial molecular features of 3,3′-diindolylmethanes essential for potent antileishmanial activity. These compounds also exhibited promising antifungal activity against *Cryptococcus neoformans*, wherein fluorophenyl substituted 3,3′-diindolylmethanes were found to be most potent antifungal agents. Developed synthetic protocol will be useful for economical and eco-friendly synthesis of potent antileishmanial and antifungal 3,3′-diindolylmethane class of compounds.

1. Introduction

Parasitic diseases such as malaria, leishmaniasis, trypanosomiasis affect millions of people worldwide and pose a major health problem in developing countries [1,2]. Amongst these malaria and leishmaniasis have affected major population with increasing number of new cases each year. Leishmaniasis is caused by protozoan parasites that belong to the genus *Leishmania* and is transmitted by the bite of certain species of sand fly (subfamily Phlebotominae). Most of the current drugs used to treat parasitic diseases are decades old and have many limitations, including the emergence of drug resistance. For leishmaniasis, either the first-line pentavalent antimonials or second-line drugs such as amphotericin B are available, which are costly and have serious side-effects, and are getting resistant to pathogens after treatment for several weeks, and hence there is a need for new antileishmanial agents with improved efficacy and less side-effects for both visceral and cutaneous leishmaniasis [3,4].

Bisindole class of compounds are known to possess diverse range of pharmacological activities such as anticancer [5–7], antimicrobial [8–11] etc. Hamacanthin A (**1**), a bisindole alkaloid isolated from the sponge *Hamacantha* sp [11] and *Spongosorites* sp [8] showed potent antibacterial activity against *Staphylococcus aureus* and MRS with MIC of 6.45 μM and antifungal activity against *Bacillus subtilis* with MIC of 3.22 μM [8]. Furthermore, bisindoles have also been reported as fluorescent molecular probes [12] of biological interest. Amongst various antileishmanial scaffolds reported, indole alkaloids [13–18] such as **2**–**3** [18] showed promising activity against *Leishmania* parasite. Munoz et al. [18] observed that dimeric indole alkaloids showed better antibacterial and antileishmanial activities compared to monomeric indole alkaloids. Dimeric alkaloids conodurine **2** and *N*-demethylconodurine **3** showed strong activity against the intracellular amastigote form of *Leishmania*. Furthermore, 3,3′-diindolylmethane (DIM, **4**) is a

☆ IIIM communication number. IIIM/1532/2013.

* Corresponding authors. Tel.: +91 191 2569111; fax: +91 191 2569333.
** Corresponding author. Medicinal Chemistry Division, Indian Institute of Integrative Medicine (CSIR), Canal Road, Jammu 180001, India. Tel.: +91 191 2569111; fax: +91 191 2569333.
E-mail addresses: sbharate@iiim.ac.in (S.B. Bharate), baldevsingh@iiim.ac.in (B. Singh), ram@iiim.ac.in (R.A. Vishwakarma).

0223-5234/$ – see front matter © 2013 Elsevier Masson SAS. All rights reserved.
http://dx.doi.org/10.1016/j.ejmech.2013.02.024

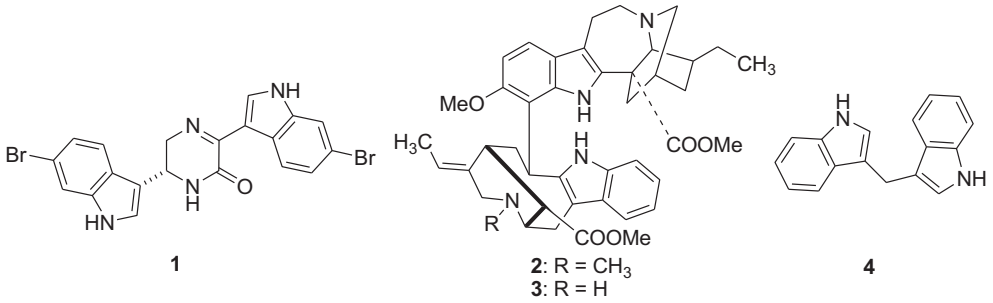

Fig. 1. Structures of biologically active bisindole alkaloids **1**–**4**.

cancer chemopreventive agent present in cruciferous vegetables such as broccoli, brussels sprouts, cabbage and kale [5]. Structures of bisindole alkaloids **1**–**4** are shown in Fig. 1.

Due to promising pharmacological activities [7,19,20] of bisindoles or diindolylmethanes, plenty of synthetic methods are available in literature for their synthesis; however most of these methods involves treatment of indoles with aldehydes in presence of homogeneous acid catalysts or Lewis acids [21–24] and only few reports on the use of heterogeneous catalysts such as inorganic-supported polyoxometalates [25], polyaniline–bismoclite composite [26] and zeolites [27,28]. Despite these reports, development of a hazard-free, waste-free, and energy-efficient synthetic protocol will be of great use for economical synthesis of this class of compounds. In continuation to our efforts toward development of efficient synthetic methodologies for preparation of biologically important scaffolds [29–31], and our efforts in the area of indole chemistry [32–35], herein we have developed an efficient protocol (Fig. 2) for preparation of potent antileishmanial 3,3′-diindolylmethanes.

2. Results and discussion

2.1. Synthesis of 3,3′-diindolylmethanes

Keeping in mind earlier findings that requirement of acidity is essential for the preparation of 3,3′-diindolylmethanes, we explored Fe-PILC catalysts **A** and **B** varying in their surface acidity. Reaction between 1*H*-indole (**5a**) and 4-hydroxy benzaldehyde (**6a**) was used as a model reaction (Table 1). Solvent optimization studies revealed that methylene chloride and water were best solvents producing higher yields. Catalyst loading as low as 15 mol% was found to be efficient producing excellent yields of products. Further, catalyst **B** was found to be better as compared to catalyst **A**. Thus catalyst **B** and water as reaction medium at room temperature were chosen for further scope exploration studies. Furthermore, we compared the reactivity of Fe-PILC **B** with plane montmorillonite clay K10 (entries 9 and 10). Product **7a** was not formed using clay K10 after 6 h of reaction time (entry 9), however ~30% product was formed when reaction was continued for 16 h (entry 10). These results clearly indicate the significant enhancement of catalytic activity of clay after pillaring it with iron.

Next, we studied scope of the reaction for various substituted indoles and different aldehydes. Treatment of indole (**5a**) with various substituted aryl and heteroaryl aldehydes in water in presence of 15 mol% of Fe-PILC **B** produced corresponding 3,3′-diindolylmethanes **7a**–**7o** in excellent yields as shown in Fig. 3. Indoles substituted with electron withdrawing group (e.g. Iodo, Fig. 4) as well as electron donating group (e.g. OMe, Fig. 5) on treatment with various aryl and heteroaryl aldehydes produced corresponding 3,3′-diindolylmethanes in excellent yields as shown in Figs. 4 and 5. Similarly aldehydes with both electron donating as well as electron withdrawing groups participated well in this reaction. Recyclability of the Fe-PILC **B** catalyst was checked to prove the heterogeneous nature and its repeated use. Treatment of 1*H*-indole (**5a**) and 4-hydroxy benzaldehyde (**6a**) in water in presence of 15 mol% Fe-PILC **B** led to formation of 3,3′-diindolylmethane **7a** in 85, 82, 78, 68% yield over four cycles respectively.

In order to understand the efficiency and catalytic activity as a function of catalyst composition, physical nature and surface acidity, the Fe-PILC **B** catalyst was characterized for specific surface area, temperature programmed reduction (TPR), temperature programmed desorption (TPD) and scanning electron microscopy (SEM) analysis. Surface area results evidenced that catalyst **B** is composed of fine aggregates, which was also supported by SEM analysis. Surface area for natural montmorillonite clay K10 and Fe-PILC **B** was found to be 52 $m^2\ g^{-1}$ and 102 $m^2\ g^{-1}$, indicating increase in the surface area in Fe-pillared clays. SEM analysis of Fe-PILC **B** showed that metal is randomly distributed over the support surface with flake formation, which was also supported by dispersion analysis (upto 99.4%). The average crystallite size of the metal was 11.60 Å. Further, SEM analysis also showed that Fe particles were present in the form of aggregates and not as a continuous film. Highly dispersed metal on the support is able to adsorb substrate and/or reagent to the high extent. TPD analysis showed that the Fe-PILC **B** contained enormously high surface acidity compared to the original clay montmorillonite K10. Total acidity of the catalyst was found to be 7.91 mmol NH_3/g catalyst, which was

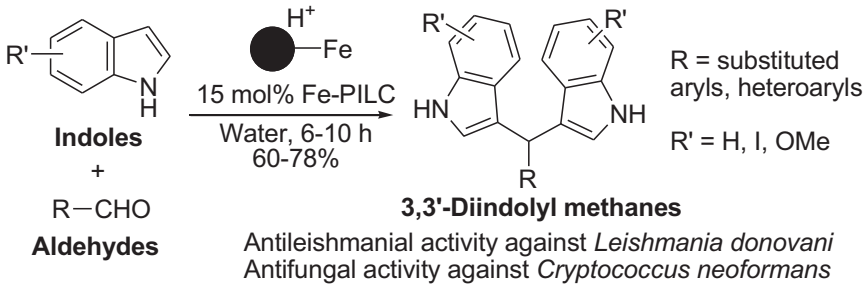

Fig. 2. Synthesis of 3,3′-diindolylmethanes using Fe-PILC catalyst.

Table 1
Optimization of reaction conditions for synthesis of 3,3′-diindolylmethanes.

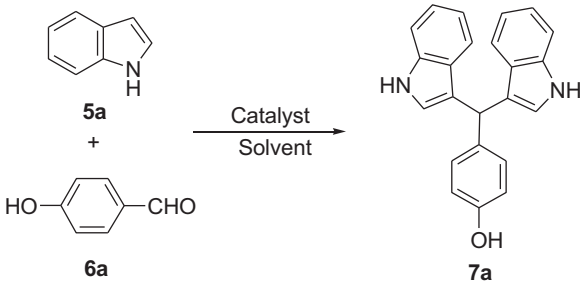

Entry	Catalyst[a]	mol%	Solvent	Temp.	Time (h)	Yield[b] (%)
1.	Fe-PILC **A**	50	CH_2Cl_2	rt	4	58
2.	Fe-PILC **A**	50	Water	rt	4	54
3.	Fe-PILC **A**	50	Water	60 °C	6	58
4.	Fe-PILC **B**	50	CH_2Cl_2	rt	4	75
5.	Fe-PILC **B**	50	Water	rt	4	70
6.	Fe-PILC **B**	50	Water	60 °C	6	76
7.	Fe-PILC **B**	30	Water	rt	6	76
8.	Fe-PILC **B**	15	Water	rt	6	74
9	Clay K10	50	Water	rt	6	0
10	Clay K10	50	Water	rt	16	30
11.	None	–	CH_2Cl_2	rt	10	0
12.	None	–	Water	rt	10	0

[a] Fe-PILC **A** and **B** vary in their surface acidity. Fe-PILC **B** is more acidic than Fe-PILC **A**.
[b] Isolated yield after silica gel column chromatography.

distributed on the surface of the clay support as 47% (3.75 mmol NH_3/g catalyst), 18% (1.40 mmol NH_3/g catalyst) and 35% (2.76 mmol NH_3/g catalyst) of weak, medium and strong acidic sites. Further, a H_2-temperature-programmed reduction (TPR) profile of the Fe-PILC **B** indicated that iron oxides gets reduced to Fe in three steps. Initially Fe_2O_3 gets reduced to Fe_3O_4 at 415 °C, which

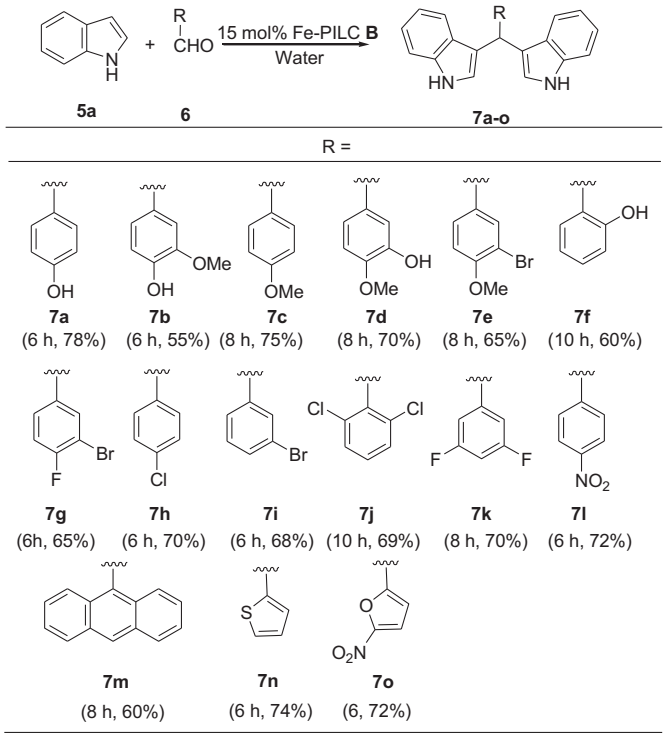

Fig. 3. Synthesis of 3,3′-diindolylmethanes **7a**–**o**.

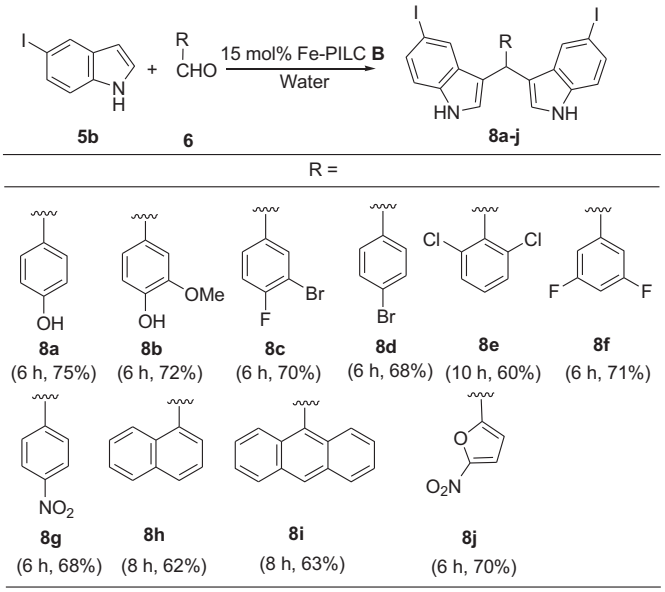

Fig. 4. Synthesis of 5,5′-diiodo-3,3′-diindolylmethanes **8a**–**j**.

further gets reduced to FeO and then consequently to Fe at 470 °C (Figure S1 of supplementary information).

2.2. Biological evaluation

All synthesized 3,3′-diindolylmethanes were evaluated for antileishmanial, antimalarial, antibacterial and antifungal, activities. The *in vitro* antileishmanial activity of 3,3′-diindolylmethanes was tested against a culture of both *Leishmania donovani* promastigotes and axenic amastigotes. Several compounds showed promising antileishmanial activity as depicted in Table 2. Amongst all tested analogs, 5-nitrofuryl substituted 5,5′-diiodo 3,3′-diindolylmethane **8j** was found to be most promising compound against *L. donovani* promastigotes showing IC_{50} and IC_{90} values of 3.02 and 6.22 μM which was comparable to control drug pentamidine. However, the 4-nitrophenyl substituted 5,5′-diiodo 3,3′-diindolylmethane **8g** showed potent activity against both promastigotes as well as amastigotes with IC_{50} values of 7.88 and 8.37 μM, respectively. Analysis of structure–activity relationship revealed that 3,3′-diindolylmethanes substituted with nitro-substituted aromatic (e.g. **7l**, **8g**, **9g**) or heteroaromatic moiety (e.g. **7o**, **8j**) showed potent antileishmanial activity against *L. donovani* promastigotes and amastigotes.

All compounds were also evaluated for *in vitro* antimalarial activity against chloroquine-sensitive (D6) and resistant (W2) clones of *Plasmodium falciparum* via determination of plasmodial LDH activity [36]. 2,6-Dichlorophenyl linked 3,3′-diindolylmethane **7j** showed antimalarial activity against D6 clone of *P. falciparum* with IC_{50} value of 12.1 μM. None of the 3,3′-diindolylmethane showed cytotoxicity towards mammalian kidney fibroblasts (vero) cells at concentration upto 4.6 μg/mL.

The antibacterial activity was tested against *S. aureus*, methicillin-resistant *S. aureus, Mycobacterium intracellulare*, *Escherichia coli* and *Pseudomonas aeruginosa*. Susceptibility of these microorganisms (except *M. intracellulare*) to test compounds was determined according to a modified version of CLSI methods [37–39]. Susceptibility of *M. intracellulare* was done using the modified Alamar Blue procedure [40]. Ciprofloxacin was used as positive control for comparison. Results of antibacterial activity are shown in Table 3. All tested diindolylmethanes were active only against

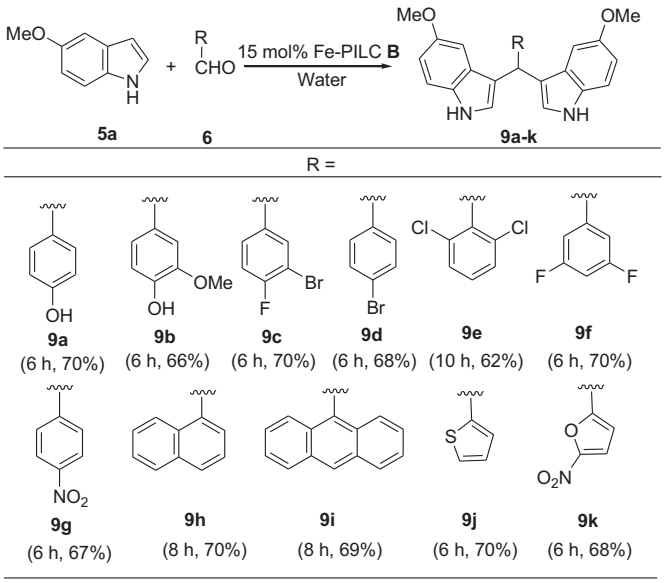

Fig. 5. Synthesis of 5,5′-dimethoxy-3,3′-diindolylmethanes **9a**–**k**.

S. aureus and methicillin-resistant *S. aureus*. Amongst tested compounds, hydroxyphenyl substituted 5,5′-diiodo-diindolylmethanes **8a** and **8b** showed most potent antibacterial activity against *S. aureus* and MRS with MIC values in the range of 2.0–4.3 μM. 3,5-Difluorophenyl substituted 3,3′-diindolylmethane **7k** also showed potent antibacterial activity against *S. aureus* and MRS with MIC values of 3.49 and 6.98 μM respectively. Only two 3,3′-diindolylmethanes **7o** and **9c** showed activity against *M. intracellulare* with IC_{50} values of 52.9 and 39.6 μM respectively.

Antifungal activities were evaluated against a panel of pathogenic fungi (*Candida albicans*, *Cryptococcus neoformans*, *Aspergillus fumigatus*) associated with opportunistic infections. Amphoterecin B was used as positive control for comparison. Several compounds showed promising activity against *C. neoformans*, however no activity was found against other fungi. Fluorophenyl substituted 3,3′-diindolylmethanes **7g** and **7k** showed potent antifungal activity against *C. neoformans* with MIC values of 2.99 and 3.49 μM respectively. Hydroxyphenyl substituted 5,5′-diiodo-diindolylmethanes **8a** which showed potent antibacterial activity, also exhibited promising antifungal activity against *C. neoformans* with MIC of 4.24 μM. Antifungal activity of 3,3′-diindolylmethanes against *C. neoformans* is shown in Table 4.

Table 2
Antileishmanial activity of 3,3′-diindolylmethanes against *Leishmania donovani* promastigotes and amastigotes.

Entry	*L. donovani* (IC_{50}/IC_{90})[a,b]		Entry	*L. donovani* (IC_{50}/IC_{90})[a,b]	
	Promastigotes	Amastigotes		Promastigotes	Amastigotes
7a	92.84/106.4	51.33/88.88	**8e**	na/na	na/na
7b	85.95/98.86	75.00/na	**8f**	24.25/41.25	23.18/44.49
7c	89.03/105.5	na/na	**8g**	7.88/10.16	8.37/38.37
7d	84.97/95.63	42.17/79.46	**8h**	na/na	na/na
7e	82.86/na	na/na	**8i**	na/na	na/na
7f	41.15/75.74	95.86/na	**8j**	3.02/6.22	25.32/28.93
7g	17.63/22.94	47.54/74.52	**9a**	81.06/90.98	42.89/76.31
7h	26.66/39.04	41.97/76.97	**9b**	na/na	na/na
7i	27.45/59.38	35.85/75.58	**9c**	15.75/46.55	47.62/66.82
7j	80.72/90.79	48.41/81.54	**9d**	32.70/58.46	na/na
7k	8.35/19.78	67.40/95.61	**9e**	na/na	na/na
7l	15.94/54.33	40.79/72.26	**9f**	26.79/65.31	49.64/78.71
7m	82.04/91.90	53.44/na	**9g**	12.08/18.81	14.73/64.22
7n	100.4/na	70.21/101.28	**9h**	66.55/82.85	33.19/na
7o	6.61/12.18	31.54/41.82	**9i**	34.65/64.92	39.83/na
8a	19.07/53.20	39.76/52.46	**9j**	38.07/65.85	59.02/84.82
8b	20.77/37.94	31.58/47.24	**9k**	37.27/59.98	na/na
8c	9.84/18.22	18.25/31.43	Pentamidine	3.29/6.21	2.9/14.3
8d	4.49/8.47	13.14/46.58	Amphotericin B	0.17/0.35	0.13/0.37

na, not active.
[a] Values are in μM.
[b] IC_{50} and IC_{90} are sample concentrations that inhibit 50% and 90% growth of *L. donovani* parasites compared to solvent controls.

2.3. Pharmacophore model for antileishmanial 3,3′-diindolylmethanes

A pharmacophore based QSAR model [41,42] was established for antileishmanial 3,3′-diindolylmethanes in order to understand the key molecular features essential for antileishmanial activity against *L. donovani* promastigotes. As depicted in Fig. 6, the selected pharmacophore model comprises two H-bond donors and four aromatic ring features. Developed model showed excellent statistical parameters, thus guaranties its utility to design new promising antileishmanial 3,3′-diindolylmethanes.

3. Conclusion

In summary, we have developed simple and efficient green protocol for preparation of structurally diverse 3,3′-diindolylmethanes. Nitroaryl substituted 3,3′-diindolylmethanes were potent antileishmanial agents possessing activity comparable to pentamidine. 3,3′-Diindolylmethanes also showed promising antibacterial and antifungal activities. Fluorophenyl substituted 3,3′-diindolylmethanes were found to be most potent antifungal compounds against *C. neoformans*. Thus, herein we have shown that developed synthetic protocol is highly efficient for economical synthesis of potent antifungal and antileishmanial diindolylmethanes. Furthermore, a developed statistically significant pharmacophore model can be used for designing potent antileishmanial 3,3′-diindolylmethanes.

4. Experimental section

4.1. General

All chemicals were obtained from Sigma–Aldrich Company and used as received. ^{1}H, ^{13}C and DEPT NMR spectra were recorded on Bruker-Avance DPX FT-NMR 500 and 400 MHz instruments. Chemical data for protons are reported in parts per million (ppm) downfield from tetramethylsilane and are referenced to the residual proton in the NMR solvent ($CDCl_3$, 7.26 ppm). Carbon nuclear magnetic resonance spectra (^{13}C NMR) were recorded at 125 MHz or 100 MHz: chemical data for carbons are reported in parts per million (ppm, δ scale) downfield from referenced to the carbon resonance of the solvent ($CDCl_3$, 77 ppm). ESI-MS and HRMS spectra were recorded on Agilent 1100 LC-Q-TOF and HRMS-6540-UHD machines. IR spectra were recorded on Perkin–Elmer IR spectrophotometer. Melting points were recorded on digital melting point apparatus.

4.2. General procedure for synthesis of 3,3′-diindolylmethanes using Fe-PILC B catalyst

To the solution of indole **5a**–**c** and aldehyde **6** in water was added 15 mol% Fe-PILC **B** and reaction mixture was stirred at room temperature for 6–10 h. Completion of the reaction was monitored by TLC. After completion of reaction, reaction mixture was filtered and filtrate was concentrated on vacuo rotavapor to get crude product. Crude product was purified by silica gel (#100–200) column chromatography to get 3,3′-diindolylmethanes **7a**–**k**, **8a**–**j**

Table 3
Antibacterial activity of 3,3′-diindolylmethanes.

Entry	IC_{50}/MIC/MBC[a]		
	S. aureus	MRS	*M. intracellulare*
7a	10.47/29.59/na	17.81/59.2/na	na/na/na
7c	9.06/na/na	na/na/na	na/na/na
7d	7.47/13.59/na	12.3/27.2/na	na/na/na
7e	7.84/na/na	31.5/na/na	na/na/na
7f	17.19/59.2/na	36.2/na/na	na/na/na
7g	3.76/5.98/na	9.23/23.9/na	na/na/na
7h	3.79/7.02/na	6.12/14.0/56.2	na/na/na
7i	3.75/12.5/na	6.30/12.5/na	na/na/na
7j	2.36/6.41/51.3	na/na/na	na/na/na
7k	2.32/3.49/na	2.93/6.98/na	na/na/na
7n	9.15/15.2/na	13.45/na/na	na/na/na
7o	12.0/28.0/28.0	8.54/14.0/na	52.9/na/na
8a	2.10/4.24/33.9	1.15/2.12/10	na/na/na
8b	1.89/4.03/na	2.11/4.03/na	na/na/na
8j	7.52/16.4/16.4	11.28/32.8/na	na/na/na
9c	3.45/10.5/na	4.67/na/na	39.6/41.8/na
9e	7.51/na/na	17.16/na/na	na/na/na
9f	4.05/11.71/na	6.89/11.7/na	na/na/na
9h	39.7/na/na	na/na/na	na/na/na
Ciprofloxacin	0.39/1.51/1.51	0.39/1.51/1.51	1.0/1.51/3.02

[a] Values are in μM.

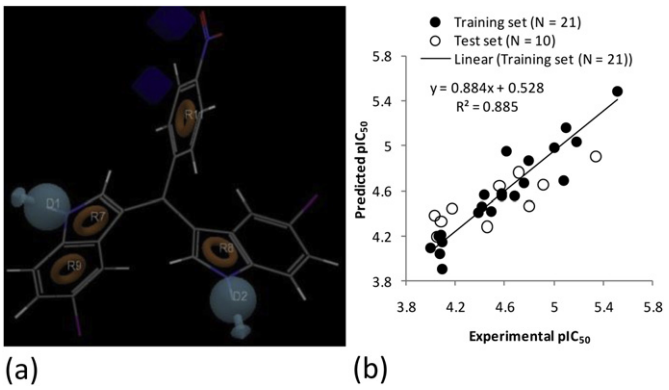

Fig. 6. Pharmacophore model for antileishmanial 3,3′-diindolylmethanes. (a) The best phase hypothesis DDRRRR.116 superimposed on one of the most active compound **8g**. In the figure a, '**D**' denotes H-bond donor and '**R**' denotes aromatic ring. (b) Correlation graph between experimental and PHASE predicted antileishmanial activity (# of PLS factors = 3; r^2 = 0.885; SD = 0.158; F = 43.8; p = 3.3 × 10^{-8}; stability = 0.529; RMSE = 0.2658; Q^2 = 0.592; pearson r = 0.836). Training: Test = 65: 35. Test set included **7a**, **7c**, **7i**, **7m**, **8a**, **8d**, **9c**, **9g**, **9h** and **9i**. All remaining analogs were part of training set.

and **9a**–**k** in 60–78% yields. Compounds **7a** [26,43], **7b** [26–28], **7c** [27,28,43–45], **7d** [46], **7f** [47], **7h** [22,25–28,44,48], **7j** [47], **7k** [49], **7l** [22,25,26,43–45], **7m** [46,50], **7n** [43], **7o** [43], **8f** [49], **9d** [51], **9f** [49] and **9g** [52] were characterized by comparison of their spectral data with literature values. Spectral data for new compounds is provided below.

*4.2.1. 3,3′-(4-Methoxy-3-bromophenyl-methanediyl)-bisindole (**7e**)*

Black solid; m.p. 104–106 °C; ^{1}H NMR ($CDCl_3$, 400 MHz): δ 7.86 (s, 2H), 7.46 (d, J = 12 Hz, 1H), 7.35–7.30 (m, 4H), 7.16–7.11 (m, 3H), 6.96 (t, J = 7.2 Hz, 2H), 6.76 (d, J = 8.4 Hz, 1H), 6.58 (s, 2H), 5.74 (s, 1H), 3.73 (s, 3H); ^{13}C NMR ($CDCl_3$, 125 MHz): δ 154.11, 137.92, 136.71, 133.33, 128.44, 126.85, 123.60, 121.90, 119.76, 119.39, 111.84, 111.69, 111.04, 56.28, 38.88; IR ($CHCl_3$): ν_{max} 3411, 2929, 1604, 1509, 1456, 1300, 1216 cm^{-1}; ESI-MS: m/z 431 $[M+1]^+$; HRMS: m/z 429.0595 calcd for $C_{24}H_{19}BrN_2O$ − H^+ (429.0597).

*4.2.2. 3,3′-(4-Fluoro-3-bromo-phenylmethanediyl)-bisindole (**7g**)*

Maroon colored solid; m.p. 102–104 °C; ^{1}H NMR ($CDCl_3$, 400 MHz): δ 7.90 (s, 2H), 7.50–7.45 (dd, J = 2.4, 6.8 Hz, 1H), 7.37 (t, J = 7.9 Hz, 4H), 7.25–7.17 (m, 3H), 6.97–6.90 (m, 3H), 6.59 (d, J = 1.6 Hz, 2H), 5.78 (s, 1H); ^{13}C NMR ($CDCl_3$, 100 MHz): δ 158.52, 156.38, 141.53, 136.70, 133.44, 129.09, 129.03, 126.75, 123.59, 122.20, 120.73, 119.69, 119.48, 118.92, 116.17, 115.97, 111.16, 102.65, 39.30; IR ($CHCl_3$): ν_{max} 3401, 1574, 1384, 1044 cm^{-1}; ESI-MS: m/z 419.0376 $[M+1]^+$, 457.0693 $[M + K]^+$; HRMS: m/z 417.03937 and 419.03801 calcd for $C_{23}H_{16}BrFN_2$ − H^+ (417.03972 and 419.03794).

Table 4
Antifungal activity of 3,3′-diindolylmethanes against *C. neoformans*.

Entry	IC_{50}[a]	MIC[a]	MFC[a]
7a	18.91	29.59	59.17
7c	35.45	na	na
7d	16.88	27.17	27.17
7f	14.64	59.17	na
7g	1.94	2.99	5.98
7h	5.56	14.04	14.04
7i	5.33	12.50	12.50
7k	2.32	3.49	3.49
7n	18.93	30.49	30.49
7o	29.64	na	na
8a	1.80	4.24	4.24
8b	3.92	32.26	na
8c	16.78	29.85	29.85
8d	5.58	30.67	30.67
9f	18.35	47.85	na
Amphotericin B	0.85	1.35	1.35

[a] Values are in μM.

*4.2.3. 3,3′-(3-Bromophenyl-methanediyl)-bisindole (**7i**)*

Black solid; m.p. 84–86 °C; ^{1}H NMR ($CDCl_3$, 400 MHz): δ 7.87 (brs, 2H), 7.43 (s, 1H), 7.38–7.34 (m, 4H), 7.30–7.24 (m, 2H), 7.20–7.11 (m, 3H), 7.07 (t, J = 7.5 Hz, 2H), 6.58 (s, 2H), 5.78 (s, 1H); ^{13}C NMR ($CDCl_3$, 125 MHz): δ 146.50, 136.61, 131.68, 129.80, 129.30, 127.39, 126.78, 123.69, 122.38, 122.05, 119.77, 119.40, 118.88, 110.84, 39.89; IR ($CHCl_3$): ν_{max} 2912, 1612, 1509, 1455, 1217, 1039 cm^{-1}; ESI-MS: m/z 401 $[M+1]^+$; HRMS: m/z 401.0457 calcd for $C_{23}H_{17}BrN_2$+H^+ (401.0474).

*4.2.4. 5,5′-Diiodo-3,3′-(4-hydroxyphenyl-methanediyl)-bisindole (**8a**)*

Dark maroon solid; m.p. 93–95 °C; ^{1}H NMR ($CDCl_3$, 400 MHz): δ 7.97 (s, 2H), 7.67 (d, J = 1.2 Hz, 2H), 7.43–7.40 (q, J = 1.6, 8.4 Hz, 2H), 7.15–7.12 (q, J = 5.6, 8.4 Hz, 4H), 6.77 (d, J = 6.8 Hz, 2H), 6.58 (d, J = 1.6 Hz, 2H), 5.67 (s, 1H), 4.73 (brs, 1H, OH); ^{13}C NMR ($CDCl_3$, 125 MHz): δ 153.67, 135.42, 134.22, 130.70, 129.31, 129.01, 128.44, 124.11, 119.08, 115.23, 112.95, 82.46, 38.62; IR ($CHCl_3$): ν_{max} 3422, 2927, 1612, 1596, 1510, 1454, 1215, 1094 cm^{-1}; ESI-MS: m/z 588.8 $[M - 1]^+$; HRMS: m/z 588.9251 calcd for $C_{23}H_{16}I_2N_2O$ − H^+ (588.9268).

*4.2.5. 5,5′-Diiodo-3,3′-(4-hydroxy-3-methoxyphenyl-methanediyl)-bisindole (**8b**)*

^{1}H NMR ($CDCl_3$, 400 MHz): δ 8.00 (s, 2H), 7.69 (d, J = 1.2 Hz, 2H), 7.42–7.39 (q, J = 1.6, 8.4 Hz, 2H), 7.13 (d, J = 8.8 Hz, 2H), 6.83 (t, J = 8.4 Hz, 2H), 6.72 (q, J = 1.6, 8.0 Hz, 1H), 6.56 (d, J = 1.6 Hz, 2H), 5.67 (s, 1H), 3.76 (s, 3H); IR ($CHCl_3$): ν_{max} 3422, 2927, 1612, 1596, 1510, 1454, 1315, 1094 cm^{-1}; ESI-MS: m/z 618.8 $[M - 1]^+$; HRMS: m/z 618.9362 calcd for $C_{24}H_{18}I_2N_2O_2$ − H^+ (618.9374).

*4.2.6. 5,5′-Diiodo-3,3′-(4-fluoro-3-bromophenyl-methanediyl)-bisindole (**8c**)*

Brown crystalline solid; m.p. 145–147 °C; ^{1}H NMR ($CDCl_3$, 400 MHz): δ 8.02 (s, 2H), 7.87 (s, 1H), 7.53 (m, 2H), 7.21–7.02 (m, 6H), 6.75 (s, 2H), 5.71 (s, 1H); ^{13}C NMR ($CDCl_3$, 100 MHz): δ 158.78, 156.82, 140.58, 140.55, 135.75, 133.17, 130.17, 129.10, 128.85, 127.65,

124.67, 117.97, 116.40, 116.22, 113.49, 113.25, 109.10, 108.93, 83.15, 38.80; IR ($CHCl_3$): ν_{max} 3428, 2924, 1595, 1490, 1455, 1243, 1045 cm^{-1}; ESI-MS: *m/z* 668.8 $[M-1]^+$; HRMS: *m/z* 670.8299 calcd for $C_{23}H_{14}BrFI_2N_2 + H^+$ (670.8312).

4.2.7. 5,5′-Diiodo-3,3′-(4-bromophenyl-methanediyl)-bisindole (**8d**)

Brown solid; m.p. 122–123 °C; ^1H NMR ($CDCl_3$, 400 MHz): δ 7.94 (s, 2H), 7.59 (d, *J* = 1.2 MHz, 2H), 7.38–7.34 (m, 4H), 7.10–7.07 (m, 4H) 6.52 (d, *J* = 1.6 Hz, 2H), 5.53 (s, 1H); ^{13}C NMR ($CDCl_3$, 125 MHz): δ 142.13, 135.75, 131.53, 130.62, 130.26, 129.24, 128.36, 124.37, 120.34, 118.18, 113.19, 83.06, 39.23; IR ($CHCl_3$): ν_{max} 3421, 2922, 1596, 1457, 1413, 1021 cm^{-1}; ESI-MS: *m/z* 650.8 $[M-H]^+$; HRMS: *m/z* 650.8407 calcd for $C_{23}H_{15}BrI_2N_2 - H^+$ (650.8424).

4.2.8. 5,5′-Diiodo-3,3′-(2,6-dichlorophenyl-methanediyl)-bisindole (**8e**)

Maroon colored solid; m.p. 247–249 °C; ^1H NMR ($CDCl_3$, 400 MHz): δ 7.98 (s, 2H), 7.57 (s, 2H), 7.38–7.33 (m, 3H), 7.14–7.08 (m, 4H), 6.74 (s, 2H), 6.59 (s, 1H); ^{13}C NMR ($CDCl_3$, 125 MHz): δ 137.68, 136.45, 135.41, 130.38, 129.55, 128.11, 128.31, 125.17, 114.66, 113.01, 83.12, 36.69; IR ($CHCl_3$): ν_{max} 3412, 2926, 1623, 1582, 1483, 1453, 1210 cm^{-1}; ESI-MS: *m/z* 640.8 $[M-H]^+$; HRMS: *m/z* 650.8526 calcd for $C_{23}H_{14}Cl_2I_2N_2 - H^+$ (650.8540).

4.2.9. 5,5′-Diiodo-3,3′-(4-nitrophenyl-methanediyl)-bisindole (**8g**)

Orange crystalline solid; m.p. 144–146 °C; ^1H NMR ($CDCl_3$, 400 MHz): δ 8.18 (d, *J* = 8.0 Hz, 2H), 8.10 (s, 2H), 7.66 (d, *J* = 1.2 Hz, 2H), 7.49–7.43 (m, 4H), 7.22 (d, *J* = 8.4 Hz, 2H), 6.63 (d, *J* = 1.6 Hz, 2H), 5.88 (s, 1H); ^{13}C NMR ($CDCl_3$, 125 MHz): δ 150.80, 146.79, 135.77, 130.91, 129.37, 128.17, 124.40, 123.83, 117.21, 113.34, 83.28, 39.72; IR ($CHCl_3$): ν_{max} 3391, 2923, 1617, 1401, 1022 cm^{-1}; ESI-MS: *m/z* 617.9 $[M-H]^+$, 641.9 $[M+Na]^+$; HRMS: *m/z* 617.9173 calcd for $C_{23}H_{15}I_2N_3O_2 - H^+$ (617.9170).

4.2.10. 5,5′-Diiodo-3,3′-(naphth-1-yl-methanediyl)-bisindole (**8h**)

Maroon solid; m.p. 224–226 °C; ^1H NMR ($CDCl_3$, 400 MHz): δ 8.05 (d, *J* = 8.0 Hz, 1H), 7.99 (brs, 2H), 7.91 (d, *J* = 8.0 Hz, 1H), 7.78 (d, *J* = 8.0 Hz, 1H), 7.70 (d, *J* = 1.2 Hz, 2H), 7.50–7.36 (m, 4H), 7.32 (t, *J* = 8.0 Hz, 2H), 7.18–7.13 (m, 3H), 6.51 (s, 1H), 6.51 (d, *J* = 2.4 Hz, 1H); ^{13}C NMR ($CDCl_3$, 100 MHz): δ 138.60, 135.85, 134.06, 131.65, 130.55, 129.47, 128.74, 128.36, 127.40, 126.04, 125.92, 125.44, 125.06, 124.13, 118.46, 113.18, 83.04, 35.54; IR ($CHCl_3$): ν_{max} 3389, 1621, 1384, 1038 cm^{-1}; ESI-MS: *m/z* 623 $[M-1]^+$; HRMS: *m/z* 622.9475 calcd for $C_{27}H_{18}I_2N_2 - H^+$ (622.9476).

4.2.11. 5,5′-Diiodo-3,3′-(anthracen-10-yl-methanediyl)-bisindole (**8i**)

Brown solid; m.p. 121–123 °C; ^1H NMR ($CDCl_3$, 500 MHz): δ 8.54–8.48 (m, 2H), 8.05–7.90 (m, 4H), 7.68 (s, 1H), 7.50–7.25 (m, 7H), 7.12 (d, 5.2 Hz, 4H), 6.73 (s, 1H), 6.71 (s, 1H); ^{13}C NMR (DMSO, 100 MHz): δ 135.10, 134.67, 133.13, 132.75, 130.77, 129.35, 128.89, 128.66, 128.31, 127.72, 126.88, 123.66, 120.13, 117.01, 112.16, 111.57, 82.02, 81.78, 33.38; IR ($CHCl_3$): ν_{max} 3416, 2927, 1622, 1582, 1483, 1453, 1210, 1172, 1028 cm^{-1}; ESI-MS: *m/z* 673 $[M-1]^+$; HRMS: *m/z* 672.9621 calcd for $C_{31}H_{20}I_2N_2 - H^+$ (672.9632).

4.2.12. 5,5′-Diiodo-3,3′-(5-nitrofuran-2-yl-methanediyl)-bisindole (**8j**)

Green crystalline solid; m.p. 121–123 °C; ^1H NMR ($CDCl_3$, 400 MHz): δ 8.15 (s, 2H), 7.75 (s, 2H), 7.52 (m, 2H), 7.21 (t, *J* = 4 Hz, 1H), 7.20 (d, *J* = 8.4 Hz, 2H), 6.91 (d, *J* = 2.4 Hz, 2H), 6.28 (d, *J* = 3.2 Hz, 1H), 5.86 (s, 1H); ^{13}C NMR ($CDCl_3$, 125 MHz): δ 160.19, 135.63, 130.98, 128.63, 127.90, 124.15, 113.62, 113.46, 112.78, 110.83, 83.45, 34.40; IR ($CHCl_3$): ν_{max} 3418, 2924, 1584, 1455, 1242, 1019, 516 cm^{-1}; ESI-MS: *m/z* 608 $[M-H]^+$; HRMS: *m/z* 607.8965 calcd for $C_{21}H_{13}I_2N_3O_3 - H^+$ (607.8963).

4.2.13. 5,5′-Dimethoxy-3,3′-(4-hydroxyphenyl-methanediyl)-bisindole (**9a**)

Dark maroon solid; m.p. 140–142 °C; ^1H NMR ($CDCl_3$, 400 MHz): δ 7.76 (s, 2H), 7.36–7.17 (m, 4H), 6.85–6.79 (m, 4H), 6.76 (d, *J* = 7.6 Hz, 2H), 6.65 (d, *J* = 1.6 Hz, 2H), 5.70 (s, 1H), 4.70 (brs, 1H, OH), 3.69 (s, 6H); IR ($CHCl_3$): ν_{max} 3409, 2927, 1581, 1482, 1439, 1204, 1038 cm^{-1}; ESI-MS: *m/z* 397.2 $[M-H]^+$; HRMS: *m/z* 397.1541 calcd for $C_{25}H_{22}N_2O_3 - H^+$ (397.1547).

4.2.14. 5,5′-Dimethoxy-3,3′-(4-hydroxy-3-methoxyphenyl-methanediyl)-bisindole (**9b**)

Dark violet solid; m.p. 88–90 °C; ^1H NMR ($CDCl_3$, 400 MHz): δ 7.83 (s, 2H), 7.25 (m, 2H), 6.87 (m, 7H), 6.65 (d, *J* = 1.6 Hz, 2H), 5.69 (s, 1H), 3.75 (s, 3H), 3.70 (s, 6H); IR ($CHCl_3$): ν_{max} 3401, 2957, 2927, 2856, 1736, 1584, 1459, 1267, 1171, 1030 cm^{-1}; ESI-MS: *m/z* 427 $[M-1]^+$; HRMS: *m/z* 427.1654 calcd for $C_{26}H_{24}N_2O_4 - H^+$ (427.1652).

4.2.15. 5,5′-Dimethoxy-3,3′-(4-fluoro-3-bromophenyl-methanediyl)-bisindole (**9c**)

Maroon solid; m.p. 93–95 °C; ^1H NMR ($CDCl_3$, 400 MHz): δ 7.78 (brs, 2H), 7.46 (dd, *J* = 2.0, 6.8 Hz, 1H), 7.27–7.23 (m, 3H), 6.98 (t, *J* = 8.4 Hz, 1H), 6.79 (d, *J* = 2.4 Hz, 2H), 6.70 (s, 2H), 6.58 (s, 2H), 5.64 (s, 1H), 3.64 (s, 6H); ^{13}C NMR ($CDCl_3$, 100 MHz): δ 158.80, 156.37, 153.89, 141.47, 133.47, 131.90, 129.09, 127.21, 124.45, 118.47, 116.15, 112.10, 108.81, 101.82, 55.92, 39.36; IR ($CHCl_3$): ν_{max} 3412, 2928, 1584, 1623, 1487, 1210, 1043, 1022 cm^{-1}; ESI-MS: *m/z* 479 $[M+1]^+$, 501 $[M+Na]^+$; HRMS: *m/z* 477.0590 calcd for $C_{25}H_{20}BrFN_2O_2 - H^+$ (477.0609).

4.2.16. 5,5′-Dimethoxy-3,3′-(2,6-dichlorophenyl-methanediyl)-bisindole (**9e**)

Cream colored solid; m.p. 217–219 °C; ^1H NMR (DMSO-d_6, 500 MHz): δ 7.88 (s, 2H), 7.33–7.28 (m, 4H), 7.16 (t, *J* = 8.0 Hz, 1H), 6.92 (s, 2H), 6.87–6.83 (m, 4H), 6.74 (s, 1H), 3.73 (s, 6H); ^{13}C NMR ($CDCl_3$, 125 MHz): δ 153.71, 138.41, 131.45, 130.01, 128.10, 127.51, 125.16, 114.72, 111.82, 111.73, 101.53, 55.75, 37.23; IR ($CHCl_3$): ν_{max} 3412, 2926, 1623, 1582, 1483, 1453, 1210 cm^{-1}; ESI-MS: *m/z* 451 $[M+1]^+$, 473 $[M+Na]^+$; HRMS: *m/z* 473.0800 calcd for $C_{25}H_{20}Cl_2N_2O_2 + Na^+$ (473.0794).

4.2.17. 5,5′-Dimethoxy-3,3′-(naphth-1-yl-methanediyl)-bisindole (**9h**)

Light brown solid; m.p. 233–235 °C; ^1H NMR ($CDCl_3$, 400 MHz): δ 8.16 (d, *J* = 8.0 Hz, 1H), 7.89 (d, *J* = 8.0 Hz, 1H), 7.80 (s, 1H), 7.75 (d, *J* = 8.0 Hz, 1H), 7.46–7.40 (m, 3H), 7.30–7.25 (m, 5H), 6.83 (t, *J* = 6.4 Hz, 4H), 6.58 (d, *J* = 2.0 Hz, 1H), 6.52 (s, 1H), 3.66 (s, 6H); ^{13}C NMR (DMSO-d_6, 100 MHz): δ 152.73, 140.24, 133.59, 131.88, 131.38, 128.50, 127.01, 126.51, 125.70, 125.47, 125.24, 124.96, 124.14, 117.31, 112.06, 110.50, 101.43, 55.29, 35.49; IR ($CHCl_3$): ν_{max} 3389, 1621, 1384, 1038 cm^{-1}; ESI-MS: *m/z* 433.2 $[M+1]^+$, 455.2 $[M+Na]^+$; HRMS: *m/z* 455.1728 calcd for $C_{29}H_{24}N_2O_2+Na^+$ (455.1730).

4.2.18. 5,5′-Dimethoxy-3,3′-(anthracen-10-yl-methanediyl)-bisindole (**9i**)

Brown solid; m.p. 123–125 °C; ^1H NMR ($CDCl_3$, 500 MHz): δ 8.65 (d, *J* = 8.9 Hz, 1H), 8.44 (s, 1H), 8.05 (brs, 2H), 7.81 (brs, 2H), 7.56–7.51 (dd, *J* = 7.2, 18.3 Hz, 1H), 7.39–7.04 (m, 8H), 6.97–6.67 (m, 4H), 6.49 (s, 1H), 3.44 (s, 6H); ^{13}C NMR ($CDCl_3$, 125 MHz): δ 153.48, 135.14, 131.57, 127.75, 127.25, 125.32, 124.68, 118.38, 112.04, 111.61, 101.80, 55.58, 34.71; IR ($CHCl_3$): ν_{max} 3416, 2927, 1622, 1582, 1483, 1453, 1210, 1172, 1028 cm^{-1}; ESI-MS: *m/z* 483.2 $[M+1]^+$, 505.2

$[M + Na]^+$, 521.2 $[M + K]^+$; HRMS: *m/z* 483.2041 calcd for $C_{33}H_{26}N_2O_2+H^+$ (483.2067).

4.2.19. 5,5′-Dimethoxy-3,3′-(thiophen-2-yl-methanediyl)-bisindole (**9j**)

Brown solid; m.p. 180–182 °C; ^{1}H NMR ($CDCl_3$, 400 MHz): δ 7.78 (s, 2H), 7.18 (d, *J* = 8.0 Hz, 2H), 7.08 (t, *J* = 4.0 Hz, 1H), 6.85 (d, *J* = 4.0 Hz, 2H), 6.81–6.75 (m, 6H), 5.98 (s, 1H), 3.64 (s, 6H); ^{13}C NMR ($CDCl_3$, 125 MHz): δ 153.81, 148.22, 131.75, 127.72, 127.20, 125.16, 123.96, 123.63, 119.27, 11.198, 11.70, 56.13, 34.79; IR ($CHCl_3$): ν_{max} 2926, 2515, 1622, 1590, 1445, 1314, 1214, 1110 cm^{-1}; ESI-MS: *m/z* 387.1 $[M - 1]^+$; HRMS: *m/z* 387.1147 calcd for $C_{23}H_{20}N_2O_2S - H^+$ (387.1162).

4.2.20. 5,5′-Dimethoxy-3,3′-(5-nitrofuran-2-yl-methanediyl)-bisindole (**9k**)

Green solid; m.p. 169–171 °C; ^{1}H NMR ($CDCl_3$, 400 MHz): δ 7.91 (s, 2H), 7.23 (m, 2H), 6.88 (s, 2H), 6.83–6.79 (m, 4H), 6.72 (s, 1H), 6.25 (d, *J* = 4.0 Hz, 1H), 5.81 (s, 1H), 3.69 (s, 6H); ^{13}C NMR ($CDCl_3$, 125 MHz): δ 160.19, 135.63, 130.98, 128.63, 127.90, 124.15, 113.62, 113.46, 112.78, 110.83, 83.45, 34.40; IR ($CHCl_3$): ν_{max} 3418, 2924, 1584, 1455, 1305, 1242, 1019 cm^{-1}; ESI-MS: *m/z* 418 $[M+1]^+$, 440 $[M + Na]^+$, 456 $[M + K]^+$; HRMS: *m/z* 418.1395 calcd for $C_{23}H_{19}N_3O_5+H^+$ (418.1398).

4.3. Fe-PILC: preparation, characterization and recyclability

Ferric chloride ($FeCl_3$) was used in Fe-PILC synthesis. A base-hydrolyzed $FeCl_3$ pillaring solution was prepared using OH/Fe molar ratio of 2.0. The hydrolysis was carried out at room temperature for 16 h under continuous stirring. Montmorillonite clay K10 powder was added gradually to Fe pillared solution, providing a required mmol of Fe per gram of clay. Fe Pillared clay suspension was stirred for 3 h at room temperature to allow ion exchange between exchangeable cations of the clay and pillar precursors. The formed PILCs were centrifuged, washed, dried in air, and calcined in air at 425 °C for 3 h.

Synthesized Fe-PILC catalyst was characterized using specific surface area determination, temperature programmed reduction (TPR), temperature programmed desorption (TPD) and scanning electron microscopy (SEM). The specific surface areas ($m^2\ g^{-1}$) of samples were estimated with the N_2 adsorption at the liquid nitrogen temperature on the Quantachrom Chem-BET 3000. Temperature programmed reduction (TPR) profiles of catalyst precursors were collected on the Quantachrom Chem-BET 3000 apparatus equipped with a thermal conductivity detector (TCD). 50 mg samples placed in a quartz U-shaped tube were reduced in 5%H_2/N_2 flow (80 mL min^{-1}) from room temperature to 700 °C at a temperature rise of 5 °C min^{-1}. Samples were pretreated in N_2 flow (50 mL min^{-1}) at 300 °C for 2 h to remove the adsorbed water and other contaminants prior to each TPR experiment.

The total acidity and acid distribution of the pillared clays was determined by ammonia TPD with the help of a CHEM BET-3000 (Quantachrome, USA) instrument in the temperature range of 30–800 °C [53]. About 0.1 g of powdered sample was taken inside a quartz U tube and degassed at 350 °C for 1 h with ultrapure helium gas. After the sample was cooled to room temperature, NH_3 gas of 1000 ppm with N_2 gas was passed through the sample for 1 h. Then the ammonia adsorbed sample was purged with helium gas at 40 °C to remove any weakly adsorbed NH_3 on the surface. The temperature-programmed desorption of ammonia was performed between 80 and 800 °C at 10 °C/min. The morphology of Fe-PILC **B** catalyst was studied using JEOL.JEM100CXII electron microscope with ASID accelerating voltage of 40 kV.

Recyclability of the Fe-PILC **B** was checked using a model reaction between 1*H*-indole (**5a**) and 4-hydroxy benzaldehyde (**6a**). To the solution of indole **5a** and aldehyde **6a** in water was added 15 mol% Fe-PILC **B** and reaction mixture was stirred at room temperature for 6 h. After completion of reaction, catalyst was recovered by filtration followed by washing with water. Recovered catalyst was dried in oven and reused in next cycle. The catalyst was recycled 3 times and the amount of catalyst recovered and percentage yield of the diindolylmethane **7a** were determined.

4.4. Assay for in vitro antileishmanial activity [54]

The assays for *in vitro* antileishmanial activity on cultures of *L. donovani* promastigotes and axenic amastigotes were carried out in 96-well plates as reported earlier [55–58]. The promastigotes culture was maintained at 26 °C in RPMI 1640 pH 7.4 with 10% FBS. The axenic amastigotes were cultured at 37 °C & 5% CO_2 in RPMI-1640 fortified with 4-morpholineethanesulfonic acid (MES) (4.88 g/L), L-glutamine (298.2 mg/L), adenosine (26.7 mg/L), folic acid (10.1 mg/L), BME vitamin mix, sodium bicarbonate (352.8 mg/L) and 10% FBS. The pH of the culture medium was 5.5. Compounds at various concentrations were added to the culture of *Leishmania* promastigotes or axenic amastigotes (2×10^6 cells/mL). Plates were incubated at 26 °C for promastigotes and 37 °C/5% CO_2 for axenic amastigotes for 72 h and growth of *Leishmania* promastigotes/amastigotes was determined by Alamar Blue Assay [54,58]. Pentamidine and amphotericin B were used as standard drugs. IC_{50} values were computed from growth inhibition curves.

4.5. Assay for in vitro antimalarial activity [36]

The assay is based on the determination of plasmodial LDH activity. For the assay, a suspension of red blood cells infected with D6 or W2 strains of *P. falciparum* (200 μL, with 2% parasitemia and 2% hematocrit in RPMI 1640 medium supplemented with 10% human serum and 60 μg/mL Amikacin) was added to the wells of a 96-well plate containing 10 μL of test samples diluted in medium at various concentrations. The plate was placed in a modular incubation chamber (Billups-Rothenberg, CA) flushed with a gas mixture of 90% N_2, 5% O_2, and 5% CO_2 and incubated at 37 °C, for 72 h. Parasitic LDH activity was determined by using Malstat™ reagent (Flow Inc., Portland, OR) according to the procedure of Makler and Hinrichs [36]. Briefly, 20 μL of the incubation mixture was mixed with 100 μL of the Malstat™ reagent and incubated at room temperature for 30 min. Twenty microliters of a 1:1 mixture of NBT/PES (Sigma, St. Louis, MO) was then added and the plate is further incubated in the dark for 1 h. The reaction was then stopped by the addition of 100 μL of a 5% acetic acid solution. The plate was read at 650 nm using the EL-340 Biokinetics Reader (Bio-Tek Instruments, Vermont). IC_{50} values were computed from the dose response curves. Artemisinin and chloroquine were included in each assay as the drug controls. DMSO (0.25%) was used as vehicle control [55–57].

4.6. Assay for in vitro antimicrobial activity

Microorganisms [fungi, *C. albicans* (ATCC 90028), *Candida krusei* (ATCC 6258), *Candida glabrata* (ATCC 90030), *C. neoformans* (ATCC 90113), and *A. fumigatus* (ATCC 204305) and bacteria, *S. aureus* (ATCC 29213), methicillin-resistant *S. aureus* (MRSA, ATCC 33591), *E. coli* (ATCC 35218), *P. aeruginosa* (ATTCC 27853), and *M. intracellulare* (ATCC 23068)] were obtained from ATCC. For all organisms, excluding *M. intracellulare* and *A. fumigatus*, susceptibility test was performed using a modified version of the CLSI (formerly NCCLS) methods [38,39], and optical density was used to monitor growth. Media supplemented with 5% Alamar Blue (BioSource

International) was utilized for growth detection of *M. intracellulare* [40] and *A. fumigatus* [37]. Concentrations that afford 50% inhibition (IC_{50}s) relative to controls were calculated using XLfit 4.2 software (IDBS) using fit model 201 based on duplicate readings. Minimum fungicidal or bactericidal concentrations were determined by removing 5 μL from each clear well, transferring to agar, and incubating until growth was seen. Drug controls ciprofloxacin (ICN Biomedicals, 99.3% purity) for bacteria and amphotericin B (ICN Biomedicals, 94.8% purity) for fungi were included in each assay.

4.7. Cytotoxicity assay

The *in vitro* cytotoxicity was determined against mammalian kidney fibroblasts (VERO) and kidney epithelial (LLC-PK_1) cells. The assay was performed in 96-well tissue culture-treated plates as described earlier [58]. Briefly, cells were seeded to the wells of the plate (25,000 cells/well) and incubated for 24 h. Samples were added and plates were again incubated for 48 h. The number of viable cells was determined by neutral red assay. IC_{50} values were determined from logarithmic graphs of growth inhibition versus concentration. Doxorubicin was used as a positive control, while DMSO was used as vehicle control.

Acknowledgments

RM and RRY thanks CSIR (India) for award of Senior Research Fellowship. Authors are thankful to analytical department, IIIM for NMR, MS and IR analysis of our compounds. Surendra Jain, Marsha Wright and John Trott are acknowledged for technical support in biological activity testing at NCNPR. United States Department of Agriculture (USDA), Agricultural Research Service Specific Cooperative Agreement No. 58-6408-2-0009 and US Department of Defense CDMRP grant #W81XWH-09 (BLT) are acknowledged for partial support of this work. Antifungal testing was supported by NIH, NIAID, Division of AIDS grant # AI27094.

Appendix A. Supplementary data

Supplementary data related to this article can be found at http://dx.doi.org/10.1016/j.ejmech.2013.02.024.

References

[1] A.R. Renslo, J.H. McKerrow, Drug discovery and development for neglected parasitic diseases, Nat. Chem. Biol. 2 (2006) 701–710.
[2] R. Kumar, S. Nylén, Immunobiology of visceral leishmaniasis, Front. Immunol. 3 (2012) 251.
[3] L.H. Freitas-Junior, E. Chatelain, H.A. Kim, J.L. Siqueira-Neto, Visceral leishmaniasis treatment: what do we have, what do we need and how to deliver it? Int. J. Parasitol. Drugs Drug Resist. 2 (2012) 11–19.
[4] M. Muniaraj, R. Paramasivan, T. Mariappan, N. Arunachalam, P.K. Sinha, The treatment of visceral leishmaniasis (kala-azar) in India: no obvious signs of long-term success, Trans. R. Soc. Trop. Med. Hyg. 106 (2012) 770–772.
[5] A. Castañon, A. Tristram, D. Mesher, N. Powell, H. Beer, S. Ashman, G. Rieck, H. Fielder, A. Fiander, P. Sasieni, Effect of diindolylmethane supplementation on low-grade cervical cytological abnormalities: double-blind, randomised, controlled trial, Br. J. Cancer 106 (2012) 45–52.
[6] D.K. Sharma, B. Rah, M.R. Lambu, A. Hussain, S.K. Yousuf, A.K. Tripathi, B. Singh, G. Jamwal, Z. Ahmed, N. Chanauria, A. Nargotra, A. Goswami, D. Mukherjee, Design and synthesis of novel *N,N'*-glycoside derivatives of 3,3'-diindolylmethanes as potential antiproliferative agents, Med. Chem. Commun. 3 (2012) 1082–1091.
[7] A. Kamal, Y.V.V. Srikanth, M.J. Ramaiah, M.N.A. Khan, M.K. Reddy, M. Ashraf, A. Lavanya, S.N.C.V.L. Pushpavalli, M. Pal-Bhadra, Synthesis, anticancer activity and apoptosis inducing ability of bisindole linked pyrrolo[2,1-c][1,4]benzodiazepine conjugates, Bioorg. Med. Chem. Lett. 22 (2012) 571–578.
[8] K.-B. Oh, W. Mar, S. Kim, J.-Y. Kim, T.-H. Lee, J.-G. Kin, D. Shin, C.J. Sim, J. Shin, Antimicrobial activity and cytotoxicity of bis(indole) alkaloids from the sponge *Spongosorites* sp, Biol. Pharm. Bull. 29 (2006) 570–573.
[9] M.D. Mansouri, T.J. Opperman, J.D. Williams, C. Stager, R.O. Darouiche, In vitro potency and in vivo efficacy of a novel bis-indole antimicrobial compound in reducing catheter colonization, Antimicrob. Agents Chemother. 56 (2012) 2201–2204.
[10] S.S. Mitchell, K.S. Lam, J. Grodberg, B.C. Potts, G. Tsueng, D.J. White, K.A. Reed, Bis-indole Pyrroles Useful as Antimicrobials Agents, in, US7375129, Nereus Pharmaceuticals, Inc., 2008.
[11] S.P. Gunasekera, P.J. McCarthy, M. Kelly-Borges, Hamacanthins A and B, new antifungal bis indole alkaloids from the deep-water marine sponge, *Hamacantha* Sp, J. Nat. Prod. 57 (1994) 1437–1441.
[12] R. Martinez, A. Espinosa, A. Tarraga, P. Molina, Bis(indolyl)methane derivatives as highly selective colourimetric and ratiometric fluorescent molecular chemosensors for Cu^{2+} cations, Tetrahedron 64 (2008) 2184–2191.
[13] B.B. Mishra, R.R. Kale, R.K. Singh, V.K. Tiwari, Alkaloids: future prospective to combat leishmaniasis, Fitoterapia 80 (2009) 81–90.
[14] G.S. Singh, Y.M.S.A. Al-kahraman, D. Mpadi, M. Yasinzai, Synthesis of *N*-(1-methyl-1*H*-indol-3-yl)methyleneamines and 3,3-diaryl-4-(1-methyl-1*H*-indol-3-yl)azetidin-2-ones as potential antileishmanial agents, Bioorg. Med. Chem. Lett. 22 (2012) 5704–5706.
[15] D. Staerk, E. Lemmich, J. Christensen, A. Kharazmil, C.E. Olsen, J.W. Jaroszewski, Leishmanicidal, antiplasmodial and cytotoxic activity of indole alkaloids from *Corynanthe pachyceras*, Planta Med. 66 (2000) 531–536.
[16] J.C. Delorenzi, M. Attias, C.R. Gattass, M. Abdrade, C. Rezende, A. Cunha-Pinto, A.T. Henrique, D.C. Bou-Habib, E.M. Saraiva, Antileishmanial activity of an indole alkaloid from *Peschiera australis*, Antimicrob. Agents Chemother. 45 (2001) 1349–1354.
[17] J.C.A. Tanaka, C.C.d. Silva, I.C.P. Ferreira, G.M.C. Machado, L.L. Leon, A.J.B.d. Oliveira, Antileishmanial activity of indole alkaloids from *Aspidosperma ramiflorum*, Phytomedicine 14 (2007) 377–380.
[18] V. Munoz, C. Moretii, M. Sauvain, C. Caron, A. Prozel, G. Massiot, B. Richard, L. Le Men-Olivier, Isolation of bis-indole alkaloids with antileishmanial and antibacterial activities from *Peschiera var heurkii* (Syn. *Tabernaemontana var heurkii*), Planta Med. 60 (1994) 455–459.
[19] K.V. Sashidhara, A. Kumar, M. Kumar, A. Srivastava, A. Puri, Synthesis and antihyperlipidemic activity of novel coumarin bisindole derivatives, Bioorg. Med. Chem. Lett. 20 (2010) 6504–6507.
[20] S.O. Lee, M. Abdelrahim, K. Yoon, S. Chintharlapalli, S. Papineni, K. Kim, H. Wang, S. Safe, Inactivation of the orphan nuclear receptor TR3/Nur77 inhibits pancreatic cancer cell and tumor growth, Cancer Res. 70 (2010) 6824–6836.
[21] N. Azizi, L. Torkian, M.R. Saidi, Highly efficient synthesis of bis(indolyl) methanes in water, J. Mol. Catal. A Chem. 275 (2007) 109–112.
[22] M.A. Pasha, V.P. Jayashankara, *p*-Toluenesulfonic acid (*p*-TSA) catalyzed efficient synthesis of bis(indolyl)methanes under grindstone method, J. Pharmacol. Toxicol. 1 (2006) 585–590.
[23] C. Ramesh, J. Banerjee, R. Pal, B. Das, Silica supported sodium hydrogen sulfate and amberlyst-15: two efficient heterogeneous catalysts for facile synthesis of bis- and tris(1*H*-indol-3-yl)methanes from indoles and carbonyl compounds, Adv. Synth. Catal. 345 (2003) 557–559.
[24] Farhanullah, A. Sharon, P.R. Maulik, V.J. Ram, Amberlist 15 catalyzed synthesis of indole-pyrazole based tri(hetero)arylmethanes, Tetrahedron Lett. 45 (2004) 5099–5102.
[25] H. Aliyan, R. Fazaeli, H.J. Naghash, A.R. Massah, A.R. Momeni, Z. Iravani, Bulk and supported tungstophosphoric acid as friendly, efficient, recyclable catalysts for the synthesis of bis-indolylmethanes under solvent-free conditions, Heteroatom Chem. 20 (2009) 325–331.
[26] S. Palaniappan, C. Saravanan, V.J. Rao, Synthesis of polyaniline–bismoclite composite and its function as recoverable and reusable catalyst, J. Mol. Catal. A Chem. 229 (2005) 221–226.
[27] M. Karthik, C.J. Magesh, P.T. Perumal, M. Palanichamy, B. Arabindoo, V. Murugesan, Zeolite-catalyzed ecofriendly synthesis of vibrindole A and bis(indolyl)methanes, Appl. Catal. A Gen. 286 (2005) 137–141.
[28] M. Karthik, A.K. Tripathi, N.M. Gupta, M. Palanichamy, V. Murugesan, Zeolite catalyzed electrophilic substitution reaction of indoles with aldehydes: synthesis of bis(indolyl)methanes, Catal. Commun. 5 (2004) 371–375.
[29] R. Mudududdla, S.K. Jain, J.B. Bharate, A.P. Gupta, B. Singh, R.A. Vishwakarma, S.B. Bharate, Ortho-Amidoalkylation of phenols via tandem one-pot approach involving oxazine intermediate, J. Org. Chem. 77 (2012) 8821–8827.
[30] S. Mohammed, A.K. Padala, B.A. Dar, B. Singh, B. Sreedhar, R.A. Vishwakarma, S.B. Bharate, Recyclable clay supported Cu (II) catalyzed tandem one-pot synthesis of 1-aryl-1,2,3-triazoles, Tetrahedron 68 (2012) 8156–8162.
[31] S.B. Bharate, R. Mudududdla, J.B. Bharate, N. Battini, S. Battula, R.R. Yadav, B. Singh, R.A. Vishwakarma, Tandem one-pot synthesis of flavans by recyclable silica-$HClO_4$ catalyzed Knoevenagel condensation and [4+2]-Diels–Alder cycloaddition, Org. Biomol. Chem. 10 (2012) 5143–5150.
[32] R.R. Yadav, N. Battini, R. Mudududdla, J.B. Bharate, N. Muparappu, S.B. Bharate, R.A. Vishwakarma, Deformylation of indole and azaindole-3-carboxaldehydes using anthranilamide and solid acid heterogeneous catalyst via quinazolinone intermediate, Tetrahedron Lett. 53 (2012) 2222–2225.
[33] S.B. Bharate, S. Manda, N. Mupparapu, N. Battini, R.A. Vishwakarma, Chemistry and biology of fascaplysin, a potent marine-derived CDK-4 inhibitor, Mini Rev. Med. Chem. 12 (2012) 650–664.
[34] S.B. Bharate, R.R. Yadav, S. Battula, R.A. Vishwakarma, Meridianins: marine-derived potent kinase inhibitors, Mini Rev. Med. Chem. 12 (2012) 618–631.
[35] S.B. Bharate, S. Manda, P. Joshi, B. Singh, R.A. Vishwakarma, Total synthesis and anti-cholinesterase activity of marine-derived bis-indole alkaloid fascaplysin, Med. Chem. Commun. 3 (2012) 1098–1103.

[36] M.T. Makler, D.J. Hinrichs, Measurement of the lactate dehydrogenase activity of *Plasmodium falciparum* as an measurement of parasitemia, Am. J. Trop. Med. Hyg. 48 (1993) 205–210.
[37] NCCLS, Reference Method for Both Dilution Antifungal Susceptibility Testing of Conidium Forming Filamentous Fungi, in: Proposal Standard M38-P, vol. 18, National Committee for Clinical Laboratory Standards, Wayne, 1998. p. 1039.
[38] NCCLS, Methods for Dilution Antimicrobial Susceptibility Tests for Bacteria that Grow Aerobically, in: NCCLS Document M7-A5, vol. 20, National Committee for Clinical Laboratory Standards, 2000. pp. 1–58.
[39] NCCLS, Reference Method for Broth Dilution Antifungal Susceptibility Testing of Yeasts, in: Approved Standard, second ed., vol. 22, National Committee for Clinical Laboratory Standards, 2002. pp. 1–51.
[40] NCCLS, Susceptibility Testing of Mycobacteria. Nocardia, and Other Aerobic Actinomycetes, in: Tentative Standard M24-T2, second ed., vol. 20, National Committee for Clinical Laboratory Standards, Wayne, 2000. pp. 1–81.
[41] S.B. Bharate, B. Singh, J.B. Bharate, S.K. Jain, S. Meena, R.A. Vishwakarma, QSAR and pharmacophore modeling of *N*-acetyl-2-aminobenzothiazole class of phosphoinositide-3-kinase-alpha inhibitors, Med. Chem. Res. 22 (2013) 890–899.
[42] S.B. Bharate, R.R. Yadav, R.A. Vishwakarma, QSAR and pharmacophore study of Dyrk1A inhibitory meridianin analogs as potential agents for treatment of neurodegenerative diseases, Med. Chem. 9 (2012) 152–161.
[43] A. Kamal, M.N.A. Khan, K.S. Reddy, Y.V.V. Srikanth, S.K. Ahmed, K.P. Kumar, U.S.N. Murthy, An efficient synthesis of bis(indolyl)methanes and evaluation of their antimicrobial activities, J. Enzym. Inhib. Med. Chem. 24 (2009) 559–565.
[44] M. Kidwai, N. Bura, N.K. Mishra, Niobium(V) pentachloride catalyzed efficient and highly rapid synthesis of bis(indolyl)-methanes under mild conditions, Indian J. Chem. 50B (2011) 229–232.
[45] S.J. Ji, M.F. Zhou, D.G. Gu, Z.-Q. Jiang, T.P. Loh, Efficient Fe-III-catalyzed synthesis of bis(indolyl)methanes in ionic liquids, Eur. J. Org. Chem. (2004) 1584.
[46] C.J. Magesh, R. Nagarajan, M. Karthik, P.T. Perumal, Synthesis and characterization of bis(indolyl)methanes, tris(indolyl)methanes and new diindolylcarbazolylmethanes mediated by Zeokarb-225, a novel, recyclable, ecobenign heterogeneous catalyst, Appl. Catal. A Gen. 266 (2004) 1–10.
[47] K. Niknam, M.A. Zolfigol, T. Sadabadi, A. Nejati, Preparation of indolylmethanes catalyzed by metal hydrogen sulfates, J. Iranian Chem. Soc. 3 (2006) 318–322.
[48] X.-F. Lin, S.-L. Cui, Y.-G. Wang, Mild and efficient synthesis of bisindolylmethanes catalyzed by tetrabutylammonium tribromide, Synth. Commun. 36 (2006) 3153–3160.
[49] D. Maciejewska, M. Rasztawicka, I. Wolska, E. Anuszewska, B. Gruber, Novel 3,3'-diindolylmethane derivatives: synthesis and cytotoxicity, structural characterization in solid state, Eur. J. Med. Chem. 44 (2009) 4136–4147.
[50] S.M. Vahdat, S. Khaksar, S. Baghery, Sulfonated organic heteropolyacid salts: recyclable green solid catalysts for the highly efficient and green synthesis of bis(indolyl)methanes in water, Lett. Org. Chem. 9 (2012) 138–144.
[51] D.-M. Zhang, Q.-G. Tang, C.-X. Ji, C. Guo, 3,3'-(4-Bromophenylmethanediyl) bis(5-methoxy-1H-indole), Acta Crystallogr. Sect. E E63 (2007) o81–o82.
[52] B.W. Ke, Y. Qin, Y. Wang, F. Wang, Amberlyst-catalyzed reaction of indole: synthesis of bisindolylalkane, Synth. Commun. 35 (2005) 1209–1212.
[53] B. Singh, S.K. Roy, K.P. Sharma, T.K. Goswami, Role of acidity of pillared interlayered clay (PILC) for the synthesis of pyridine bases, J. Chem. Technol. Biotechnol. 71 (1998) 246–252.
[54] J. Mikus, D. Steverding, A simple colorimetric method to screen drug cytotoxicity against *Leishmania* using the dye Alamar Blue, Parasitol. Int. 48 (2000) 265–269.
[55] M. Kumarihamy, S.I. Khan, M. Jacob, B.L. Tekwani, S.O. Duke, D. Ferreira, N.P.D. Nanayakkara, Antiprotozoal and antimicrobial compounds from the plant pathogen *Septoria pistaciarum*, J. Nat. Prod. 75 (2012) 883–889.
[56] F. Machumi, A. Yenesew, J.O. Midiwo, M. Heydenreich, E. Kleinpeter, B.L. Tekwani, S.I. Khan, L.A. Walker, I. Muhammad, Antiparasitic and anticancer carvotacetone derivatives of *Sphaeranthus bullatus*, Nat. Prod. Commun. 7 (2012) 1123–1126.
[57] A.A. Rahman, V. Samoylenko, M.R. Jacob, R. Sahu, S.K. Jain, S.I. Khan, B.L. Tekwani, I. Muhammad, Antiparasitic and antimicrobial indolizidines from the leaves of *Prosopis glandulosa var. glandulosa*, Planta Med. 77 (2011) 1639–1643.
[58] J. Mustafa, S.I. Khan, G. Ma, L.A. Walker, I.A. Khan, Synthesis and anticancer activities of FA analogs of podophyllotoxin, Lipids 39 (2004) 167–172.